

## **Multi-omics analysis to evaluate solar exposure impact on skin ecosystem and a new SPF50+ photoprotective system**

**Carine Jacques<sup>1</sup>, Emilien L. Jamin<sup>2,3</sup>, Daniel Bacqueville<sup>1</sup>, Martine Maitre<sup>1</sup>, Justin Oules<sup>1</sup>, Anais Noustens<sup>1</sup>, Isabelle Jouanin<sup>2,3</sup>, Laurent Debrauwer<sup>2,3</sup>, Sandrine Bessou-Touya<sup>1</sup> & Hélène Duplan<sup>1</sup>**

<sup>1</sup> Pierre Fabre Dermo-cosmétique, Centre R&D Pierre Fabre, Avenue Hubert Curien, Cedex 01, 31025 Toulouse, France

<sup>2</sup> MetaboHUB-MetaToul, National Infrastructure of Metabolomics and Fluxomics, Toulouse, 31077 France

<sup>3</sup> Toxalim (Research Centre in Food Toxicology), Université de Toulouse, INRAE, ENVT, INP-Purpan, UPS, 31027 Toulouse, France.

### **Corresponding author:**

Carine Jacques

Pierre Fabre Dermo-Cosmétique, Toulouse, France

Email: carine.jacques@pierre-fabre.com

Tel: +33 534506474

Fax: +33 534503425

## ABSTRACT

**Background:** Skin is the primary interface with the external environment. To evaluate the impact of external factors like sun exposure on the cutaneous ecosystem (skin-sebum-microbiota), it must be studied as a whole to understand how they interact with each other.

**Methods:** We developed a reconstructed human epidermal model colonized with human microbiota and sebum to reproduce the complexity of the skin ecosystem. This *in vitro* model was exposed to simulated solar radiation (SSR). A new SPF50+ photoprotective system containing a specific combination of four sun filters (TriAsorB, Tinosorb S, Uvinul T150 and Uvinul A+) and affording a broad spectrum UVB+A photoprotection, was evaluated on this *in vitro* model.

Metabolomic profiles were performed by means of NMR and UHPLC-HRMS. Metagenomic analyses were performed from genomic DNA extract samples. ITS1 of the ribosomal RNA gene, and of the V1-V3 region of 16S gene were sequenced by high-speed sequencing.

**Results:** Metabolomic analyses revealed high skin oxidative stress with modification of glutathione and purine pathway but also urea cycle. Other pathways have been highlighted linked to skin microbiota, like BCAAs cycle, lipid metabolism and tryptophan pathway. With the new photoprotective system, metabolome of the skin was preserved and the physiological interactions within the skin ecosystem were protected from sun exposure deleterious effects.

**Conclusion:** This study identified a highly accurate metabolomic signature of sun exposed skin in an *in vitro* model representative of a complete skin ecosystem. Metabolomic signature was correlated to the metagenomic analysis of skin microbiota and explain interactions between skin and microbiota.

**Key words:** sun-exposure, multi-omics, metabolomics, metagenomics, skin ecosystem

## **Introduction.**

As the skin is the primary interface with the external environment, the skin ecosystem consisting of our microbiota, a collection of micro-organisms such as bacteria, viruses, and fungi reflect the state of the surrounding skin ecosystem. To evaluate the impact of external factors like sun exposure, the cutaneous ecosystem, including skin, hydrolipidic film and microbiome, has to be studied as a whole to understand how they interact with each other and contribute to adaptation to external stress like sun exposure. Its impact in gut health and disease is widely accepted, but we are just starting to understand the role of cutaneous microbiota and its interaction with skin.

When chronically exposed to sun radiation, skin is not only subjected to medical endpoints like sunburn and cancer, but also influences its phenotypic appearance inducing photo-aging. Therefore, sun avoidance and the use of sunscreens are recommended to prevent these effects of major public health issue. The consequences of sun exposure have been previously documented both at genetic and proteomic levels. However, only few studies describe the contribution of sun exposure to biochemical changes that result in skin metabolome alterations, and interactions between skin and its microbiota have not been described.

Metabolomics is the most recent systems biology omics approach. It measures the abundance of various metabolites, and thus enables profiling different metabolic pathways. The metabolome is defined as all the low molecular weight compounds of endogenous nature, which are important substrates, by-products, and building blocks of many different biological processes (endo-metabolome) but also of exogenous compounds and their biotransformation by the body (xeno-metabolome). These high-throughput technologies generate high-resolution and high-quality data on the physiological and metabolic state of a target tissue. However, to date, there are very few studies of dermatological outcomes combining multiple omics measurements within the same experiment, in particular metabolomics, lipidomics, metagenomics<sup>1</sup>.

We developed a reconstructed human epidermal model colonized with skin microbiota and sebum to reproduce the complexity of the skin ecosystem. This model gets closer to the reality of the cutaneous physiology and permits to study the interactions between skin and microbiota. The *in vitro* skin ecosystem model was exposed to simulated solar radiation (SSR). A new SPF50+ photoprotective system containing a specific combination of four sun filters (TriAsorB, Tinosorb S, Uvinul T150 and Uvinul A+) and affording a broad spectrum UVB+A photoprotection (patented association WO581; WO984), was evaluated on this *in vitro* skin ecosystem model. Metabolomics profiles were performed in combination with 16S and ITS metagenomic analysis. We combine these two technologies in order to highlight the interaction between the skin and its microbiota and vice versa.

Here, we present the first study which profiled a wide range of metabolites and identified a highly accurate metabolomic signature of sun exposed skin in an *in vitro* model with complete skin ecosystem.

## **Materials and Methods**

### **Chemicals**

Chemicals and solvents (analytical grade) were purchased from the following sources: sodium chloride from Sigma-Aldrich (St Quentin Fallavier, France); ammonium acetate (Fluka, Levallois Perret France); acetonitrile and ethanol (VWR); acetic acid and methanol (Fisher Scientific, Illkirch, France). Ultrapure water, obtained using a Milli-Q system (Millipore, Saint Quentin en Yvelines, France), was used for sample extraction and preparation of HPLC mobile phases.

The SPF50+ photoprotective system used contained a specific combination of four sun filters, affording a broad spectrum UVB+A photoprotection (patented association WO581; WO984). This sunscreen contains Avène thermal spring water, C12-15 alkyl benzoate, caprylic/capric triglyceride, dicaprylyl carbonate, diethylamino hydroxybenzoyl hexyl benzoate (Uvinul A+), glycerine, ethylhexyl triazone (Uvinul T150), phenylene bis-diphenyltriazine (Triasorb), bis-ethylhexyloxyphenol methoxypenyl triazine (Tinosorb S), potassium cetyl phosphate, steryl alcohol, VP/eicosane copolymer, caprylyl glycol, glyceryl stearate, PEG-100 sterate, PPG-1-PEG-9 lauryl glycol ether, glyceryl dibehenate, xanthan gum, benzoic acid, tribehenin, polyacrylate-13, glyceryl behenate, sorbitan isocitrate, polyisobutene, tocopheryl glucoside, polysorbate 20, Red 33, and tocopherol.

### **Cutaneous ecosystem model**

Primary normal human keratinocytes, obtained from abdominal dermolipectomy of a healthy subject, were used to produce reconstructed human epidermis (RHE) on polycarbonate filters with a method derivative of the method of Frankart et al<sup>2</sup>. RHE model was colonized with skin microbiota and sebum at J13 to reproduce the complexity of the skin ecosystem. Microbiome was collected from 18 volunteers; the zone of interest was on the forehead of non-pathological volunteers (10cm<sup>2</sup>). All the samples were systematically sampled using a standardized procedure. Sebum was collected using a sampling kit developed by Synelvia (Toulouse, France). Zone of interest was on the forehead of non-pathological volunteers. After extraction, sebum amples were stored at -80°C under inert gas into ambered vials before application on RHE.

The experimental conditions tested were: (1) non-irradiated tissue models in the absence of photoprotective system; (2) Solar-irradiated RHE models in the absence of photoprotective system; (3) non-irradiated RHE models after application of the SPF50+ photoprotective system; (4) Solar-irradiated RHE models after application of the SPF50+ photoprotective system. All the conditions

were tested on 3 batches with 6 donors of microbiota and sebum per batch and condition (N=18 per condition).

SPF50+ photoprotective system were applied 1hour prior sun exposure at a dose of 2 mg/cm<sup>2</sup>. The models were irradiated with solar-simulated light (SSR) at a dose of 16.5 J/cm<sup>2</sup>. After irradiation, RHE models were incubated for a further 24 h. At the end of the experiment, the surface of RHE models were washed twice with NaCl 0.9% and then dried with a sterile dry cotton bud. The RHE models were grinded using a Fast-prep method and homogenized. Samples were frozen in liquid nitrogen and stored at -80°C until metabolomic analysis.

### **Metabolite profiling using NMR**

Samples were centrifuged (4000 g, 15 min., 4°C), and 200 µL of supernatants was transferred into 3mm inner diameter NMR tubes. <sup>1</sup>H NMR spectra were obtained at 300 K on a Bruker Avance III HD 600 MHz NMR spectrometer (Bruker Biospin, Rheinstetten, Germany), operating at 600.13 MHz for <sup>1</sup>H resonance frequency, using an inverse detection 5 mm <sup>1</sup>H-<sup>13</sup>C-<sup>15</sup>N-<sup>31</sup>P cryoprobe attached to a Cryoplatform (the preamplifier unit). Tuning and matching of the probe, lock, shims tuning, pulse (90°) and gain computation were automatically performed for each sample. <sup>1</sup>H NMR spectra were acquired using the 1D NOESY experiment. Prior to Fourier transform, an exponential line broadening function of 0.3 Hz was applied to the FID. All NMR spectra were phase- and baseline corrected and referenced to the chemical shift of TSP (0 ppm) using Topspin (V3.2, Bruker Biospin, Germany). NMR spectra were divided into fixed-size buckets (0.01 ppm) between 10 and 0.5 ppm using the AMIX software (v3.9.15, Bruker), and the area under the curve was calculated for each bucket (integration). Integrations were normalized according to the total intensity.

To confirm the chemical structures of the metabolites, 2D-homonuclear <sup>1</sup>H-<sup>1</sup>H COSY (correlation spectroscopy) and 2D-heteronuclear <sup>1</sup>H-<sup>13</sup>C HSQC (heteronuclear single quantum coherence spectroscopy) NMR spectra were also obtained for selected samples.

The structural identification of discriminant metabolites was achieved by matching 1D and 2D NMR spectra with those of authentic standards referenced in an in-house database, as well as with data obtained from an online database (HMDB (TMIC)).

### **Untargeted metabolomic analysis using RP-UHPLC-HRMS**

After NMR analyzes, samples were transferred from NMR tubes to UHPLC vials and injected in the UHPLC ACQUITY system from Waters (Manchester, UK), using water/methanol/acetic acid 95/5/0.1 (v:v:v) as mobile phase A and methanol/acetic acid 100/0.1 (v:v) as mobile phase B, at a

flow rate of 0.3 mL/min. The following gradient elution was used: 0-30 min: 0% to 100% of B, 30-34 min: 100% of B. The separation was achieved at 30°C with a Hypersil Gold C18 column (100 x 2.1 mm, 1.9 µm) from Thermo Scientific (Les Ulis, France). Typical electrospray ionization parameters were used. High resolution mass spectra were acquired with a Synapt G2-Si mass spectrometer from Waters (Manchester, UK), between *m/z* 50 and 800 in the sensitivity and the centroid modes. Samples were analyzed randomly, and a blank sample corresponding to the deuterated water used to dissolve extracts before NMR analyzes, was analyzed 11 or 6 times along the sequence of injections of RHE or HepaRG® extracts, respectively. Similarly, a QC sample corresponding to a pool of all samples, was analyzed 11 times along the sequence. Raw data were converted in mzXML format using Proteowizard and CWT and then processed with XCMS and CAMERA.

Structural identifications of discriminant metabolites were achieved on a LTQ Orbitrap XL mass spectrometer (Thermo Scientific, Les Ulis, France) coupled to U3000 (Thermo Scientific, Les Ulis, France) liquid chromatographic system. The same chromatographic parameters as for sample analyses were applied. Tandem mass spectrometry (MS/MS) analyses were targeted on [M+H]<sup>+</sup> or [M-H]<sup>-</sup> ions of discriminant metabolites and were tentatively identified according to the nomenclature of the metabolomics standards initiative <sup>3</sup>.

### **Analysis of skin microbiota**

Taxonomic identification is based on the sequencing of the ribosomal RNA gene, which is present in all microbial or fungi genomes.

After genomic DNA extraction and purification from all cells in each sample, V1-V3 region from 16S sub-unit for bacteria or intergenic spacer 1 (ITS1) between 18S and 5,8S sub-unit of ribosomal RNA genes for fungi were amplified by PCR using oligonucleotides targeting conserved regions. The sequence of each DNA fragment thus duplicated was then carried out by high-speed sequencing. The analysis of the sequences obtained and their comparison with international databases make it possible to phylogenetically identify microorganisms and fungi present in each sample in relation to already known organisms.

Barcodes and primers as well as chimeras were removed from the sequence files during the filtering steps. Sequences with 100% homology between them were grouped into unique sequences and then into OTUs (operational taxonomic units: 97% threshold) which will be identified later.

The bioinformatics analysis of the sequencing data allows the identification of microorganisms present at different taxonomic levels (phylum to genus). The analysis allowing phylogenetic affiliation up to the genus level was carried out using bioinformatics tools for the processing of large

amounts of sequence data (Mothur). The identification was carried out on the Greengenes DATA BASE taxonomy for bacteria and the Findley (2013) DATA BASE taxonomy for fungi.

Differential analysis was carried out after GMPR normalization and DEseq2 method to identify genus that were significantly more abundant in one group than the other.

### **Statistical analysis**

Principal Component Analysis (PCA) was firstly applied to check the validity of acquisition, to detect potential outliers and internal clusters. Due to the experimental design, to consider the paired structure, multilevel method <sup>4</sup> was applied. These methods combine analysis of variance and multivariate method. In the first stage, ANOVA is applied to split up total variability included in spectral data: independent matrices are associated to each experimental factor and to the interaction. In the second stage, independent matrices are simultaneously analyzed based on the multi-blocks OPLS.

## Results and Discussion

### Metabolomic analysis

Metabolomics analyses were performed in both RHE models and RHE surface wash to highlight any metabolites modulated by sun-exposure with or without application of SPF50+ photoprotective system. Principal component analyses (PCA), based on NMR or MS data show discrimination according to the irradiation and treatment factor on the metabolome. From this significant discrimination, 1025 features are discriminant ( $VIP > 1$ ) and significant (FDR corrected p-value of Mann Whitney test  $< 0.05$ ). From these discriminant features, corresponding metabolites were identified. Their fold change (log2) between each condition were measured. Only one-fold change for each identified metabolite (identification level of 1 or 2) is displayed in Table 1, corresponding to the feature with the lowest p-value and the highest fold change.

	IR. SPF50+ vs NI.SPF50+	IR.CTRL vs NI.CTRL
Octanoic acid	0.28	1.77
Lactate	ns	0.44
L-Isoleucine	ns	-1.60
L-Leucine	ns	-0.78
L-Phenylalanine	0.20	-0.18
L-Tryptophan	ns	-0.13
Succinyladenosine	-0.23	-2.45
Tyrosine	ns	2.52
Uric acid	1.27	2.62
Indoleacetic acid	ns	1.2
L-Alanine	-1.08	-2.79
L-Phenylalanine	ns	ns
Xanthine	-0.21	0.57

**Table 1.** Identified metabolites (levels 1 or 2) modulated (log2 fold change) in tryptophan and BCAA pathway in skin ecosystem model with and without SSR irradiation and SPF50+ photoprotective system analyzed by  $^1\text{H}$  NMR followed by C18-UHPLC-ESI-HRMS

A pathway enrichment analysis was conducted to explore whether sun exposure induced perturbations in specific metabolic pathways. Several pathways were modulated after sun exposition.<sup>5</sup>

Pathway enrichment and modulated metabolites showed that the skin is under high oxidative stress with modification of glutathione and purine pathway but also urea cycle. As already described *in vivo* by Randhawa et al<sup>6</sup>, the skin goes to catabolism rather than anabolism pathway, and produces higher oxidative stress. Other pathways have been highlighted, in particular linked to skin microbiota, like

BCAAs cycle, lipid metabolism and tryptophan pathway. We next focus on only two pathways: tryptophan and BCAA.

### **Tryptophan pathway**

SSR modulate Tryptophan and its metabolites, in particular indole acetic acid (Table 1). Since tryptophan cannot be produced by the human body, increase of this compound in the skin ecosystem model is related to microbiome. In the literature, it has been reported lower levels of tryptophan and indole acetic acid at the surface of the skin of atopic patients, correlated with microbiome modification. Modulation of tryptophan metabolism derived from the skin microbiota play a regulatory function in skin inflammation <sup>7–10</sup>. Indole acetic acid, a skin microbiota-derived tryptophan metabolite, negatively regulated skin inflammation in patients with atopic dermatitis, revealing that skin microbiota play a significant functional role in the pathogenesis. The tryptamine pathway in the microbiota leads to the production of the majority of indole and indole derivatives. These tryptophan metabolites act as ligands that can activate the aryl hydrocarbon receptor (AhR) on innate lymphoid cells to induce IL-22 secretion, driving the release of antimicrobial peptides (AMPs) and providing protection from infections by pathogens. Regulation of AhR activation by microbial metabolites may represent a promising strategy for the treatment of inflammatory skin disorders <sup>11</sup>.

Based on the metabolomic analysis of the skin ecosystem, we observed a significant modification of Tryptophan pathway with a decrease of tryptophan level and an increase of indole acetic acid after SSR irradiation without photoprotective system. After application of the SPF50+ photoprotective system, tryptophan and its metabolites stay at the basal level showing a protective effect of the skin ecosystem against SSR irradiation.

The essential amino acid tryptophan and its metabolites are emerging as important mediators of host–microbe interactions, with multiple effects on host physiology on the one hand, and consequences for the survival of the microorganisms, on the other hand <sup>11</sup>.

### **BCAA pathway**

When bacteria are experiencing stress, they have adaptive responses to increase survival and undergo programmed molecular responses <sup>12</sup>. For bacteria one of these stress management methods is to enhance branched-chain amino acid (BCAA) catabolism for energy production <sup>13,14</sup>.

In the *in vitro* skin ecosystem model, we observed a significant decrease in BCAA catabolites (leucine and isoleucine) after SSR irradiation without photoprotective system (Table 1). BCAA pathway was significantly disturbed by SSR irradiation and may support observations of disrupted bacterial activity. BCAAs can also be utilized by fungi for energy needs <sup>15</sup>.

When the SPF50+ photoprotective system is applied locally, the downregulation of the two main amino acids of the BCAA cycle (Isoleucine and Leucine) was no longer observed (Table 1). Recent data suggest that deficiencies of leucine and isoleucine reduce collagen synthesis in skin by suppressing the action of mTOR<sup>16</sup>. Indeed, leucine has also been used for attenuation of skin wrinkles in conjunction with glycine and proline *in vivo*<sup>17</sup>.

On the skin surface, there is a complex interplay between the host metabolism and its microbiota. It cannot be ruled out that a subset of metabolites presented above are either directly produced or are altered by the skin microflora. Indeed, skin microbiome plays an important role in maintaining cutaneous health and the skin microflora is constantly adapting its response to intrinsic and extrinsic factors. When the new photoprotective system was applied on the *in vitro* model, metabolome of the skin was preserved and the interactions between skin and its ecosystem were protected from sun exposure deleterious effects.

### Metagenomic analysis 16S and ITS.

From the 16S analysis, two main bacterial genera were significantly modified by SSR irradiation: *Burkholderia* and *Cutibacterium* genus. Both genera were significantly more abundant on microbiota after SSR irradiation without photoprotective system (Fig.1). After application of the SPF50+ photoprotective system, bacterial genera were not still modulated significantly by SSR irradiation (Fig.2).

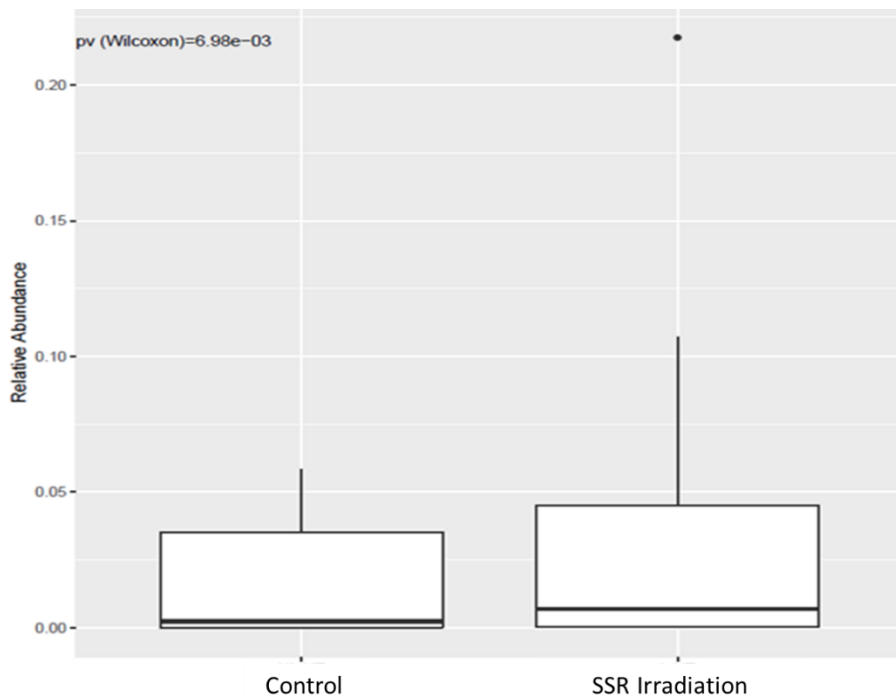


**Fig. 1.** Descriptive analysis at genus level of *Cutibacterium*: Average of relative abundance per group (SSR irradiated or not SSR irradiated *in vitro* skin ecosystem)

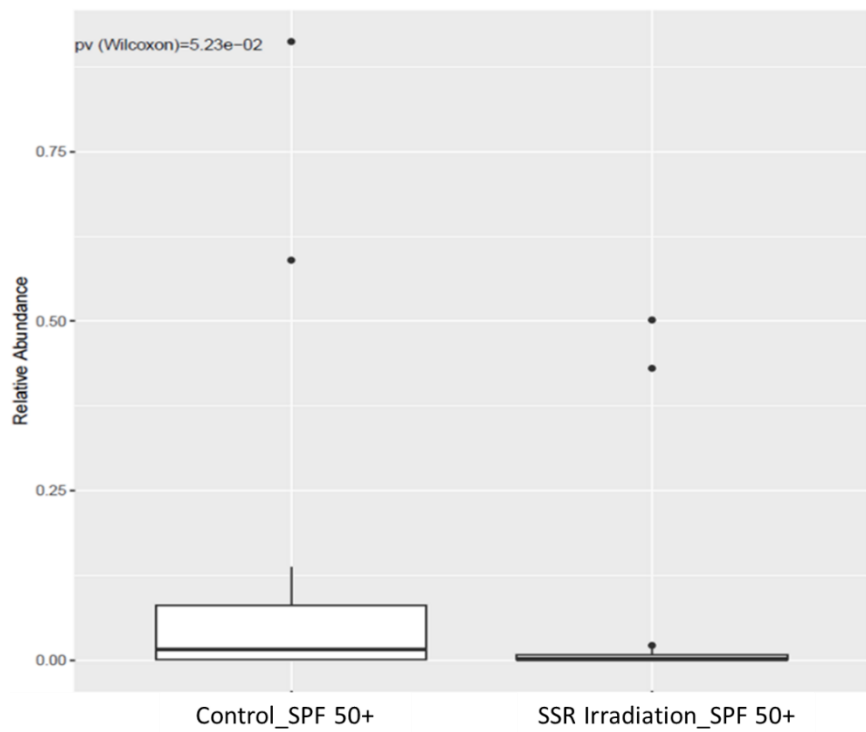


**Fig. 2.** Descriptive analysis at genus level of *Cutibacterium*: Average of relative abundance per group (SSR irradiated or not SSR irradiated *in vitro* skin ecosystem with SPF50+ photoprotective system)

*Burkholderia* and *Cutibacterium* are both anaerobic genus bacteria. *Cutibacterium*, in particular, *cutibacterium acnes* could have a role in the protection against radical oxidative stress cause by SSR irradiation by producing radical oxygenase<sup>18</sup>. A detailed analysis on *cutibacterium* species modulated could give some insight in the role of this genera to prevent SSR damage

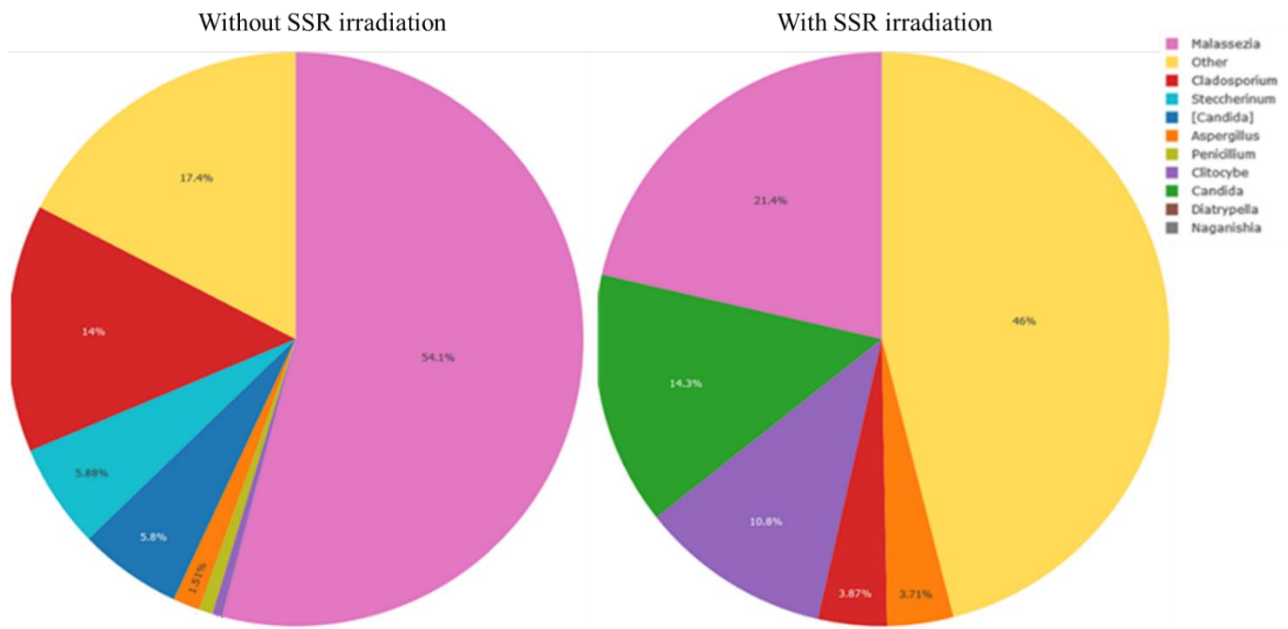


**Fig 3.** Average of relative abundance of fungi genus per group (SSR irradiated or not SSR irradiated *in vitro* skin ecosystem)

After SSR irradiation, skin fungal composition at the genus level showed some differences: *Malassezia* and *Cladosporium* genus are impacted by irradiation without photoprotective system while *Candida* and *Clitocybe* genus seem to be favored (Fig.3)

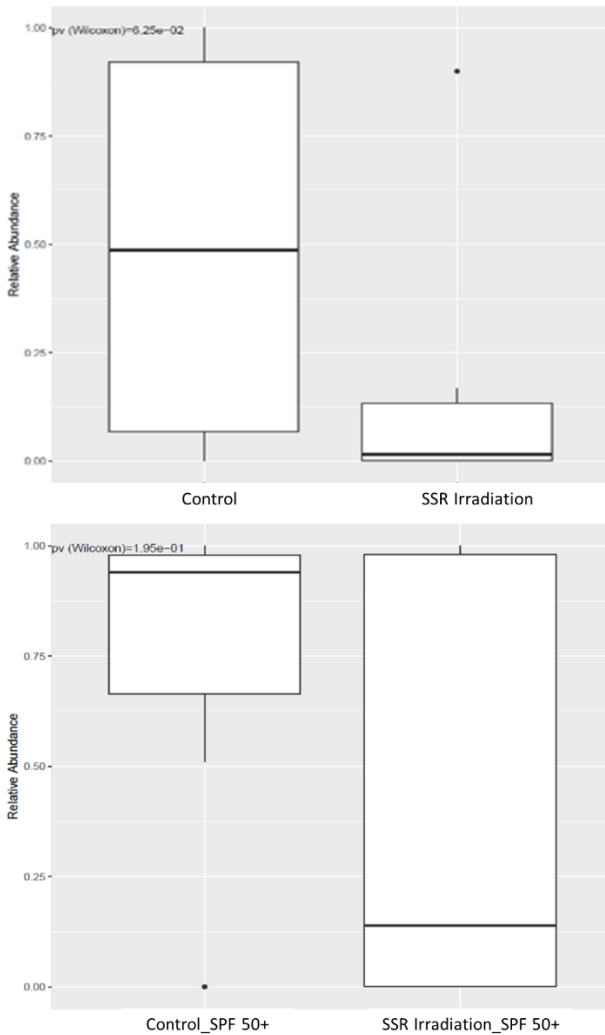


**Fig. 4.** Mustache boxes of *Malassezia* genus (SSR irradiated or not SSR irradiated *in vitro* skin ecosystem without or with SPF50+ photoprotective system).

*Malassezia* can convert tryptophan into indole compounds<sup>19</sup>. An array of bioactive indoles is produced by *Malassezia* species which are AhR ligands and may affect antifungal immune responses and pathogenesis by modulating dendritic cells function<sup>20</sup>. Gaitanis *et al.* also reported that AhR ligands produced by *Malassezia* change ROS production and modulate the inflammatory response<sup>21</sup>.

There is some evidence that *Malassezia* may sense ambient solar radiation and accordingly adapt its metabolism through differential synthesis of melanin and photoprotective indolic compounds both *in vivo* and *in vitro*. The data found on the metagenomic analysis correlate with the data obtained with the metabolomic analysis showing a modification of Tryptophan pathway that can be partly impacted due to the modification of the microbiota population at the surface of the skin.

Thus, adaptation of *Malassezia* metabolism to the level of incident SSR irradiation seems to be a biochemical mechanism that has the potential to influence the microenvironment of the neighboring skin. The ability to activate the AhR receptor and thus modulate down-stream effects places

*Malassezia* yeasts within two significant pathophysiological pathways, namely mediation of ultraviolet damage and modulation of the host immune response. These observations, together with the anatomic co-localization of *Malassezia* yeasts with basal cell carcinoma, led to the hypothesis that they could be implicated in skin carcinogenesis<sup>22,23</sup>.

## **Conclusion**

This study profiled a wide range of metabolites and identified a highly accurate metabolomic signature of sun exposed skin in an *in vitro* model with complete skin ecosystem. Metabolomic signature can be correlated to the metagenomic analysis of skin microbiota and explain interactions between skin and cutaneous microbiota.

This original *in vitro* model coupled with innovative technologies enable evaluation of photoprotection products and proved to be of great help for understanding skin ecosystem interaction.

## **Acknowledgments**

All LC-HRMS analyses were achieved at MetaToul (Toulouse metabolomics & fluxomics facilities, [www.metatoul.fr](http://www.metatoul.fr)), which is part of French National Infrastructure MetaboHUB for Metabolomics and Fluxomics [MetaboHUB-ANR-11-INBS-0010]

## **Conflict of Interest Statement**

Authors are employees of Pierre Fabre Dermo-Cosmetique, France and National Institute of Agronomic and Environment Research, France. The authors report no other conflicts of interest in this work.

## References

1. Elpa, D. P., Chiu, H.-Y., Wu, S.-P. & Urban, P. L. (2021) Skin Metabolomics. *Trends in Endocrinology & Metabolism* **32**, 66–75.
2. Frankart, A., Coquette, A., Schroeder, K.-R. & Poumay, Y. (2012) Studies of cell signaling in a reconstructed human epidermis exposed to sensitizers: IL-8 synthesis and release depend on EGFR activation. *Arch Dermatol Res* **304**, 289–303.
3. Sumner, L. W. *et al.* (2007) Proposed minimum reporting standards for chemical analysis: Chemical Analysis Working Group (CAWG) Metabolomics Standards Initiative (MSI). *Metabolomics* **3**, 211–221.
4. Liquet, B., Cao, K.-A. L., Hocini, H. & Thiébaut, R. (2012) A novel approach for biomarker selection and the integration of repeated measures experiments from two assays. *BMC Bioinformatics* **13**.
5. Cottret, L. *et al.* (2018) MetExplore: collaborative edition and exploration of metabolic networks. *Nucleic Acids Research* **46**, W495–W502.
6. Randhawa, M., Sangar, V., Tucker-Samaras, S. & Southall, M. (2014) Metabolic Signature of Sun Exposed Skin Suggests Catabolic Pathway Overweights Anabolic Pathway. *PLoS ONE* **9**, e90367.
7. Lamas, B. *et al.* (2016) CARD9 impacts colitis by altering gut microbiota metabolism of tryptophan into aryl hydrocarbon receptor ligands. *Nature Medicine* **22**, 598–605.
8. Kepert, I. *et al.* (2017) D-tryptophan from probiotic bacteria influences the gut microbiome and allergic airway disease. *Journal of Allergy and Clinical Immunology* **139**, 1525–1535.
9. Kawasaki, H. *et al.* (2014) A tryptophan metabolite, kynurenone, promotes mast cell activation through aryl hydrocarbon receptor. *Allergy* **69**, 445–452.
10. Morris, G. *et al.* (2017) The Role of the Microbial Metabolites Including Tryptophan Catabolites and Short Chain Fatty Acids in the Pathophysiology of Immune-Inflammatory and Neuroimmune Disease. *Mol Neurobiol* **54**, 4432–4451.
11. Liu, Y. *et al.* (2020) Gut Microbiome Fermentation Determines the Efficacy of Exercise for Diabetes Prevention. *Cell Metabolism* **31**, 77-91.e5.

12. Bearson, S., Bearson, B. & Foster, J. W. (2006) Acid stress responses in enterobacteria. *FEMS Microbiology Letters* **147**, 173–180.
13. Serrazanetti, D. I. *et al.* (2011) Acid Stress-Mediated Metabolic Shift in *Lactobacillus sanfranciscensis* LSCE1. *Appl Environ Microbiol* **77**, 2656–2666.
14. Neis, E., Dejong, C. & Rensen, S. (2015) The Role of Microbial Amino Acid Metabolism in Host Metabolism. *Nutrients* **7**, 2930–2946.
15. Shimizu, M. (2018) NAD+/NADH homeostasis affects metabolic adaptation to hypoxia and secondary metabolite production in filamentous fungi\*. *Bioscience, Biotechnology, and Biochemistry* **82**, 216–224.
16. Yamane, T. *et al.* (2018) Branched-chain amino acids regulate type I tropocollagen and type III tropocollagen syntheses via modulation of mTOR in the skin. *Bioscience, Biotechnology, and Biochemistry* **82**, 611–615.
17. Kawashima, M. *et al.* (2013) Improvement of crow's feet lines by topical application of 1-carbamimidoyl-L-proline (CLP). *European Journal of Dermatology* **23**, 195–201.
18. Rozas, M. *et al.* (2021) From Dysbiosis to Healthy Skin: Major Contributions of *Cutibacterium acnes* to Skin Homeostasis. *Microorganisms* **9**, 628.
19. Szelest, M., Walczak, K. & Plech, T. (2021) A New Insight into the Potential Role of Tryptophan-Derived AhR Ligands in Skin Physiological and Pathological Processes. *International Journal of Molecular Sciences* **22**, 1104.
20. Vlachos, C., Schulte, B. M., Magiatis, P., Adema, G. J. & Gaitanis, G. (2012) Malassezia-derived indoles activate the aryl hydrocarbon receptor and inhibit Toll-like receptor-induced maturation in monocyte-derived dendritic cells: Malassezia indoles activate AhR and inhibit moDC maturation. *British Journal of Dermatology* **167**, 496–505.
21. Gaitanis, G., Velegraki, A., Magiatis, P., Pappas, P. & Bassukas, I. D. (2011) Could Malassezia yeasts be implicated in skin carcinogenesis through the production of aryl-hydrocarbon receptor ligands? *Medical Hypotheses* **77**, 47–51.

22. Velegraki, A., Cafarchia, C., Gaitanis, G., Iatta, R. & Boekhout, T. (2015) Malassezia Infections in Humans and Animals: Pathophysiology, Detection, and Treatment. *PLoS Pathog* **11**, e1004523.
23. Gaitanis, G. *et al.* (2008) AhR Ligands, Malassezin, and Indolo[3,2-b]Carbazole are Selectively Produced by Malassezia furfur Strains Isolated from Seborrheic Dermatitis. *Journal of Investigative Dermatology* **128**, 1620–1625.